

Electronic Supporting Information

Binding discrepancy of fluoride in quaternary ammonium and alkali salts by a tris(amide) receptor in solid and solution-states

Sandeep Kumar Dey, Barun Datta and Gopal Das*

Department of Chemistry, Indian Institute of Technology Guwahati, Assam-781039, India

E-mail: gdas@iitg.ernet.in

Characterization of receptor L:

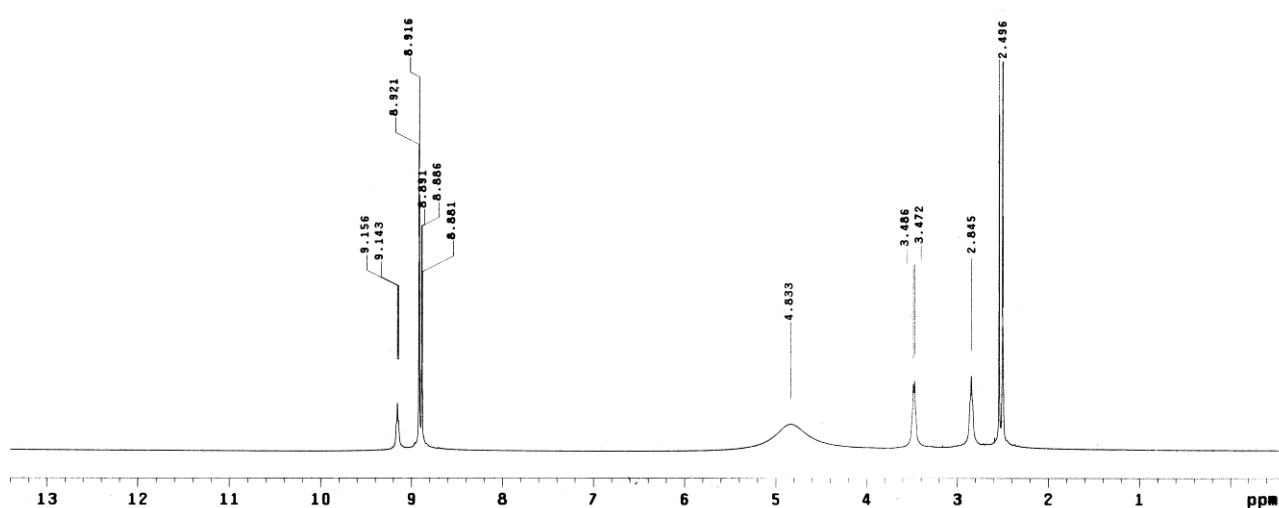


Figure S1. ¹H NMR spectrum of L in DMSO-*d*₆ at 298 K.

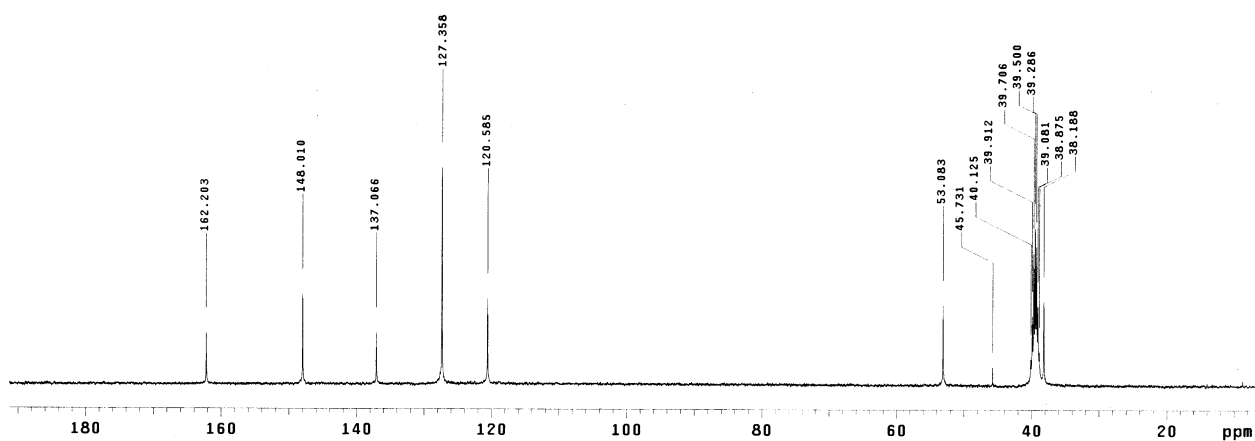


Figure S2. ¹³C NMR spectrum of L in DMSO-*d*₆ at 298 K.

Characterization of TBAF complex, **1d**:

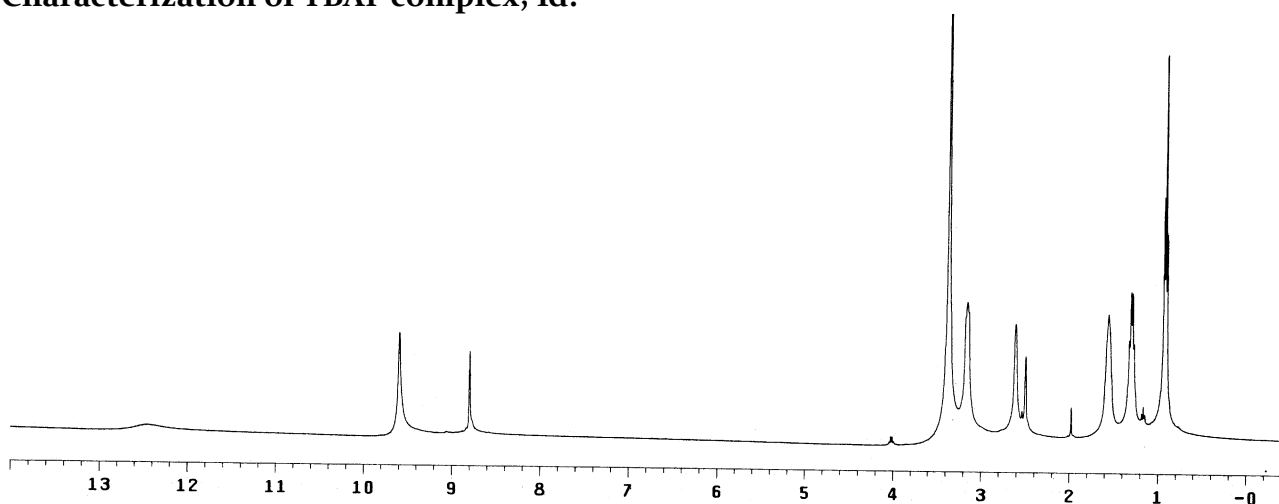


Figure S3. ¹H NMR spectrum of TBAF complex, **1d** in DMSO-*d*₆ at 298 K.

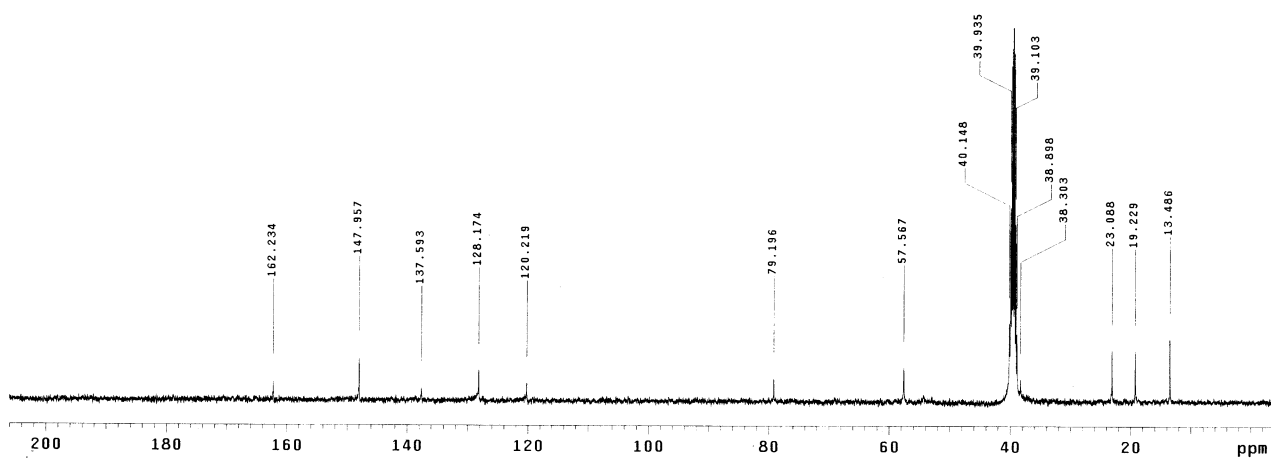


Figure S4. ¹³C NMR spectrum of TBAF complex, **1d** in DMSO-*d*₆ at 298 K.

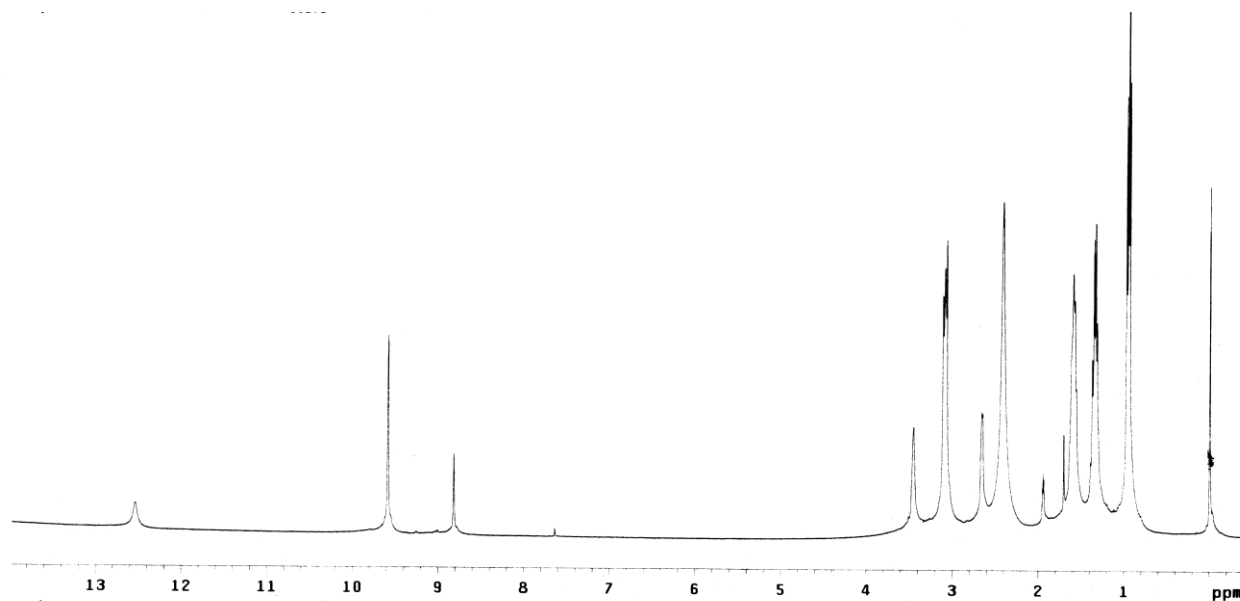


Figure S5. ¹H NMR spectrum of TBAF complex, **1d** in CD₃CN at 298 K.

Characterization of KF complex, **2**:

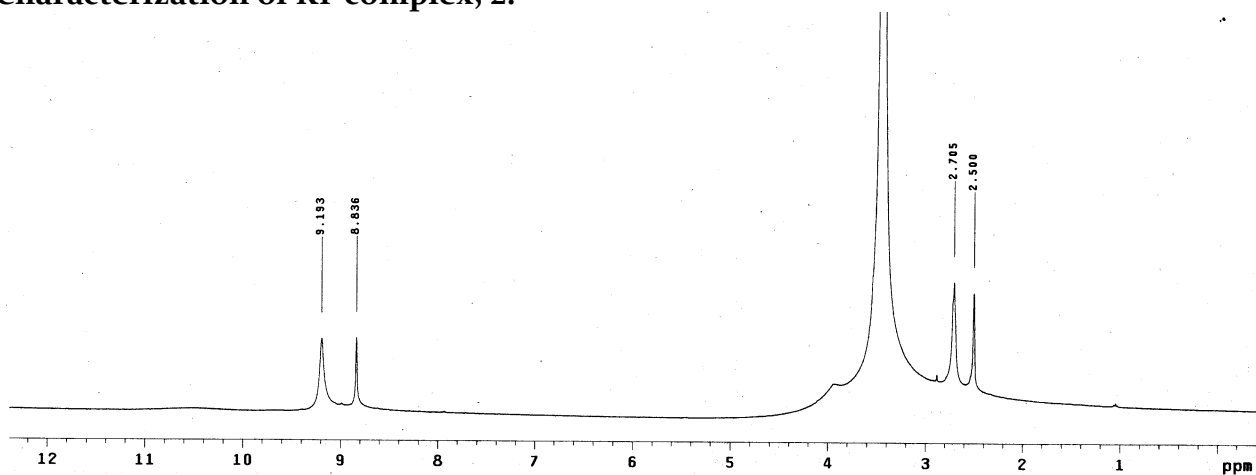


Figure S6. ¹H NMR spectrum of KF complex, **2** in DMSO-*d*₆ at 298 K.

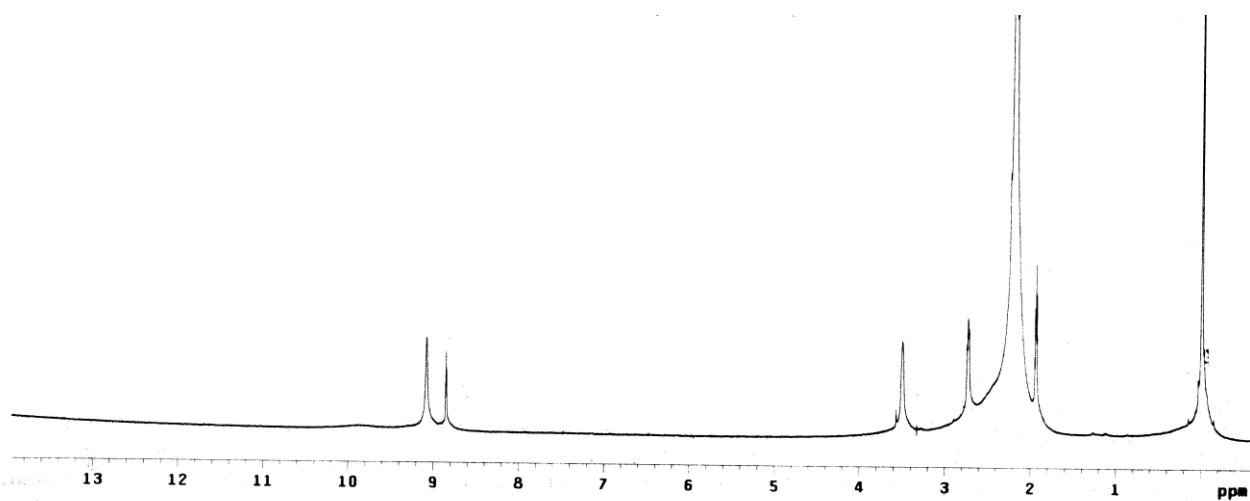


Figure S7. ¹H NMR spectrum of KF complex, **2** in CD₃CN at 298 K.

Additional Crystallographic data:

Table S1. Crystallographic parameters and refinement details of L-DMSO, L-DMF and complexes **1d** and **2**.

Parameters	L-DMSO	L-DMF	Complex 1d	Complex 2
Formula	C ₂₉ H ₃₀ N ₁₀ O ₁₆ S	C ₃₀ H ₃₁ N ₁₁ O ₁₆	C ₄₆ H ₆₀ FN ₁₁ O ₁₆	C ₂₇ H ₂₄ FKN ₁₀ O ₁₇
<i>F</i> _w	806.70	801.66	1042.05	1858.21
Crystal system	Triclinic	Monoclinic	Triclinic	Triclinic
Space group	<i>P</i> -1	<i>P</i> ₂ 1/ <i>c</i>	<i>P</i> -1	<i>P</i> -1
<i>a</i> /Å	11.2942(3)	17.2139(6)	10.1372(3)	11.2710(12)
<i>b</i> /Å	12.4744(4)	11.1890(3)	16.4160(5)	12.4543(13)
<i>c</i> /Å	12.8671(4)	25.1968(7)	17.3515(8)	12.8718(14)
α /°	84.723(2)	90.00	109.413(2)	84.825(6)
β /°	79.650(3)	131.890(2)	97.059(2)	79.744(6)
γ /°	88.404(2)	90.00	106.906(1)	88.329(6)
<i>V</i> /Å ³	1775.65(9)	3612.8(2)	2527.35(17)	1770.6(3)
<i>Z</i>	2	4	2	2
<i>D</i> _c /g cm ⁻³	1.509	1.474	1.369	1.536
μ Mo <i>K</i> α /mm ⁻¹	0.180	0.122	0.107	0.246
<i>T</i> /K	298(2)	298(2)	180(2)	298(2)
θ max.	28.29	28.390	28.270	27.140
Total no. of reflections	13679	49295	26140	26731
Independent reflections	8734	8991	9814	7784
Observed reflections	7605	4777	7233	6870
Parameters refined	520	516	683	505
<i>R</i> ₁ , <i>I</i> > 2 σ (<i>I</i>)	0.0508	0.0580	0.0645	0.0838
<i>wR</i> ₂ (all data)	0.1510	0.2115	0.2429	0.2728
GOF (<i>F</i> ²)	0.911	1.023	1.005	1.035

Table S2. Hydrogen bond interactions involved in the crystal structures of L-DMSO.

L-DMSO	D-H...A	<i>d</i> (H...A)	<i>d</i> (D...A)	<(D-H...A)
Intraligand interactions	N8-H...O6	1.94(3)	2.891(3)	167(3)
	C27-H...O6	2.46(2)	3.185(3)	134(2)
	C1g...C2g		3.756	
Interactions with lattice DMSO	N5-H...O16	1.98(3)	2.834(3)	157(2)
	C14-H...O16	2.34(2)	3.239(3)	161(2)
	O16...C2g		3.532	
Interligand interactions	N2-H...O11	1.98(3)	2.856(3)	134(2)
	C1-H...O11	2.70(2)	3.427(3)	132(1)
	C20-H...O2	2.65(2)	3.127(4)	110(2)
	C19-H...O13	2.64(2)	3.309(3)	125(2)
	C19-H...O15	2.66(2)	3.530(4)	148(2)
	O8...C24		3.169(3)	
	O5...C12		3.023(3)	
	O12...N3		2.987(3)	
	O12...O3		3.007(3)	

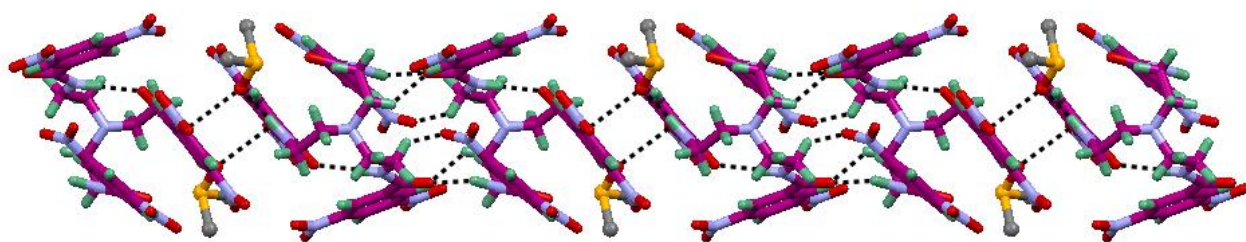


Figure S8. Solvent bridged 1D chain in L-DMSO diagonally along ac -axis.

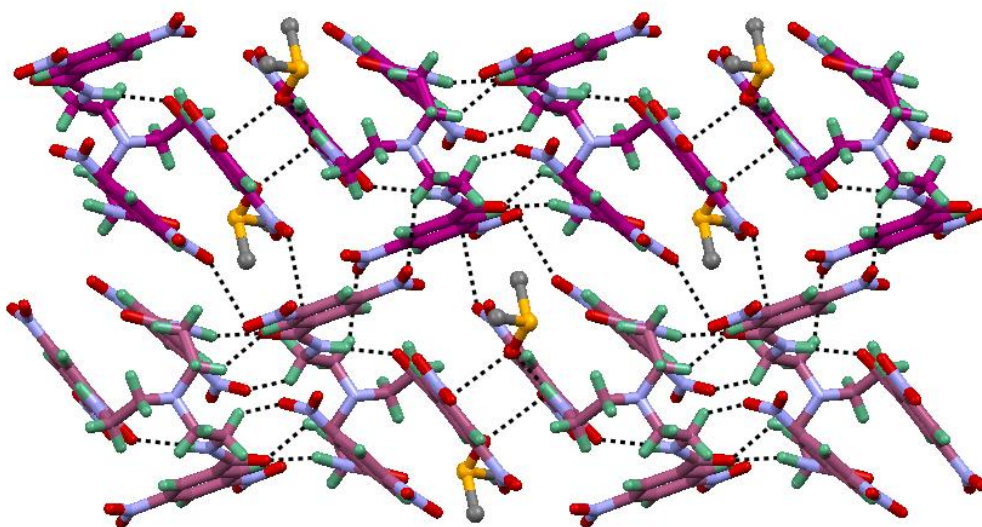


Figure S9. Crystal packing of L-DMSO as viewed down the a -axis showing the H-bonding and electron donor-acceptor interactions between two adjacent solvent-bridged 1D chains of receptor molecules.

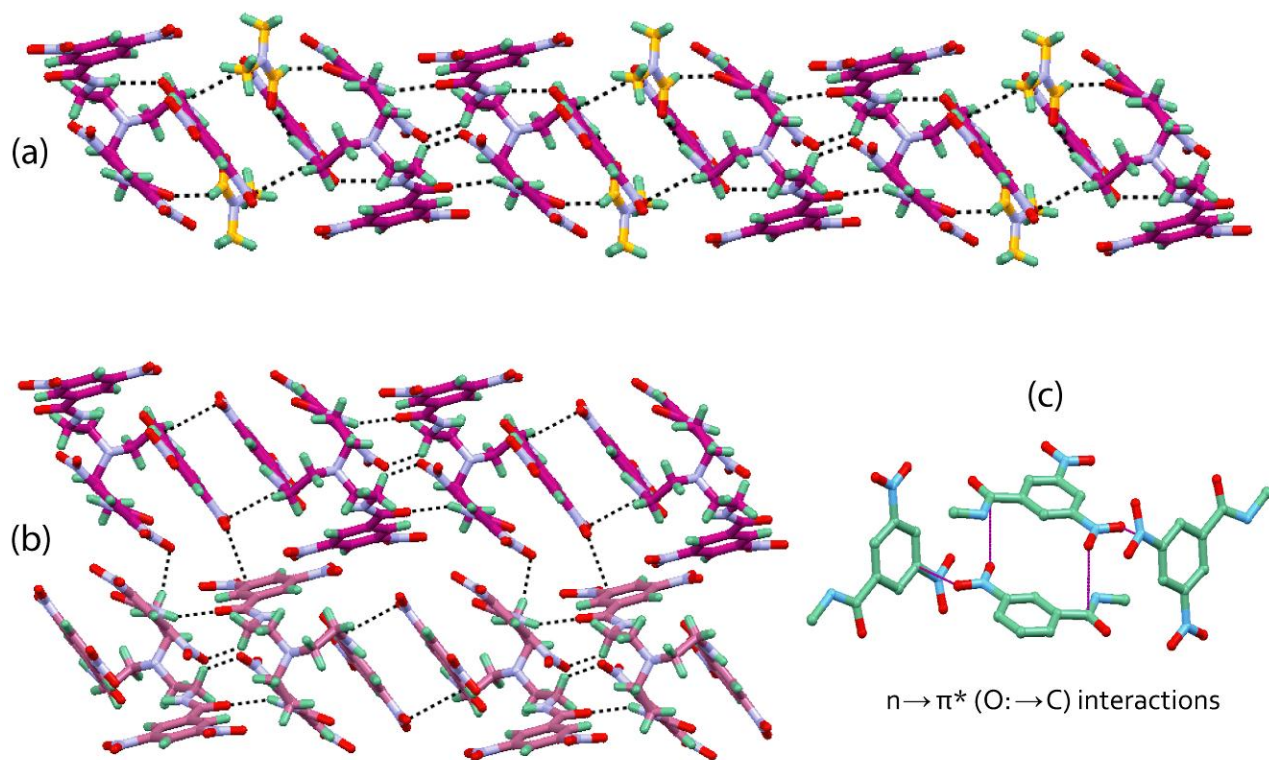


Figure S10. (a) Solvent bridged 1D chain of L-DMF along *c*-axis. (b) Crystal packing of L-DMF as viewed down the *b*-axis showing the intermolecular H-bonding and electron donor-acceptor interactions between two adjacent 1D chains of receptor molecules (Lattice DMF molecules are omitted for clarity). (c) Magnified view of the $n \rightarrow \pi^*$ ($O \rightarrow C$) electron donor-acceptor interactions between the adjacent receptor molecules in L-DMF.

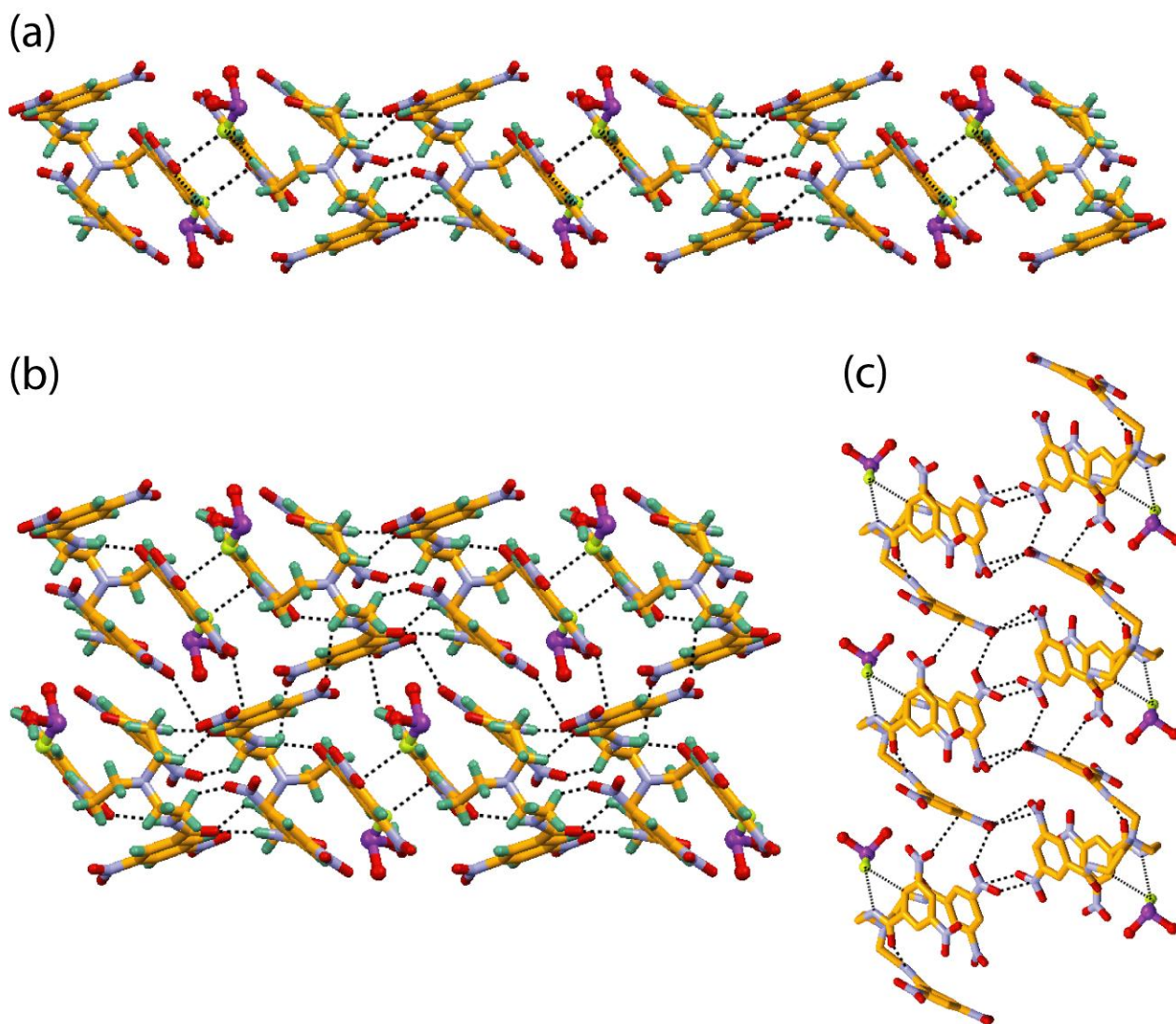


Figure S11. (a) H-bonded $\text{KF}(\text{H}_2\text{O})_2$ bridged 1D chain of **L** in **2** diagonally along ac -axis. (b) Crystal packing of **2** as viewed down the a -axis showing the H-bonding and electron donor-acceptor interactions between two adjacent 1D chains of receptor molecules. (c) View of the $n \rightarrow \pi^*$ ($\text{O} \rightarrow \text{N/C}$) electron donor-acceptor interactions between the adjacent 1D chains.

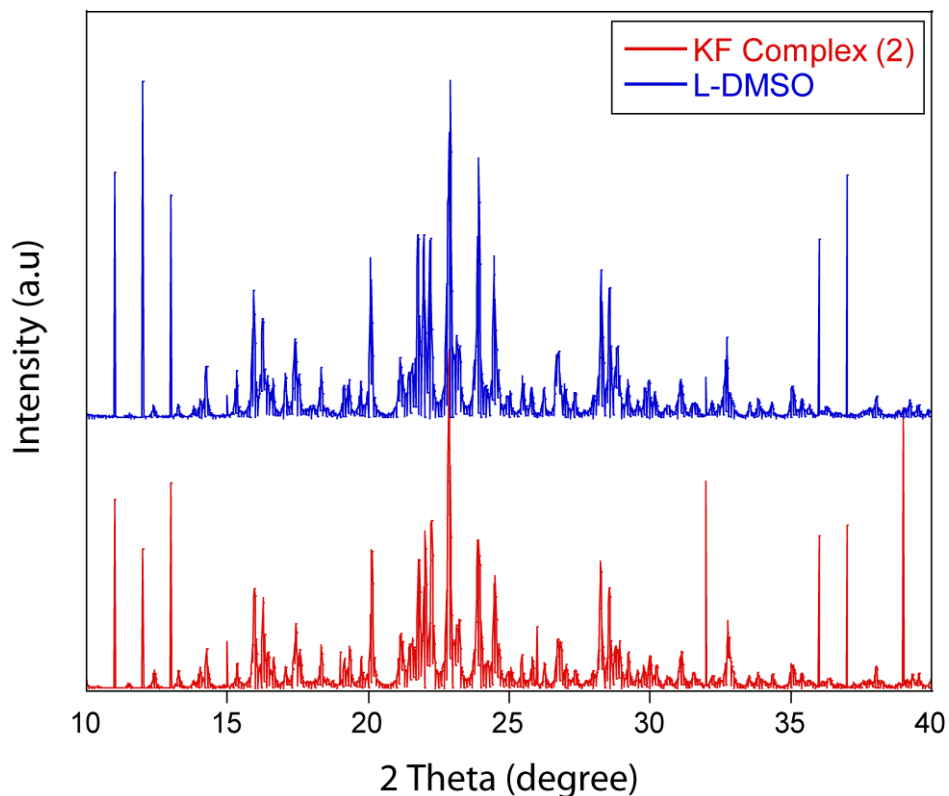


Figure S12. Simulated PXRD patterns of isostructural L-DMSO and KF complex (2).

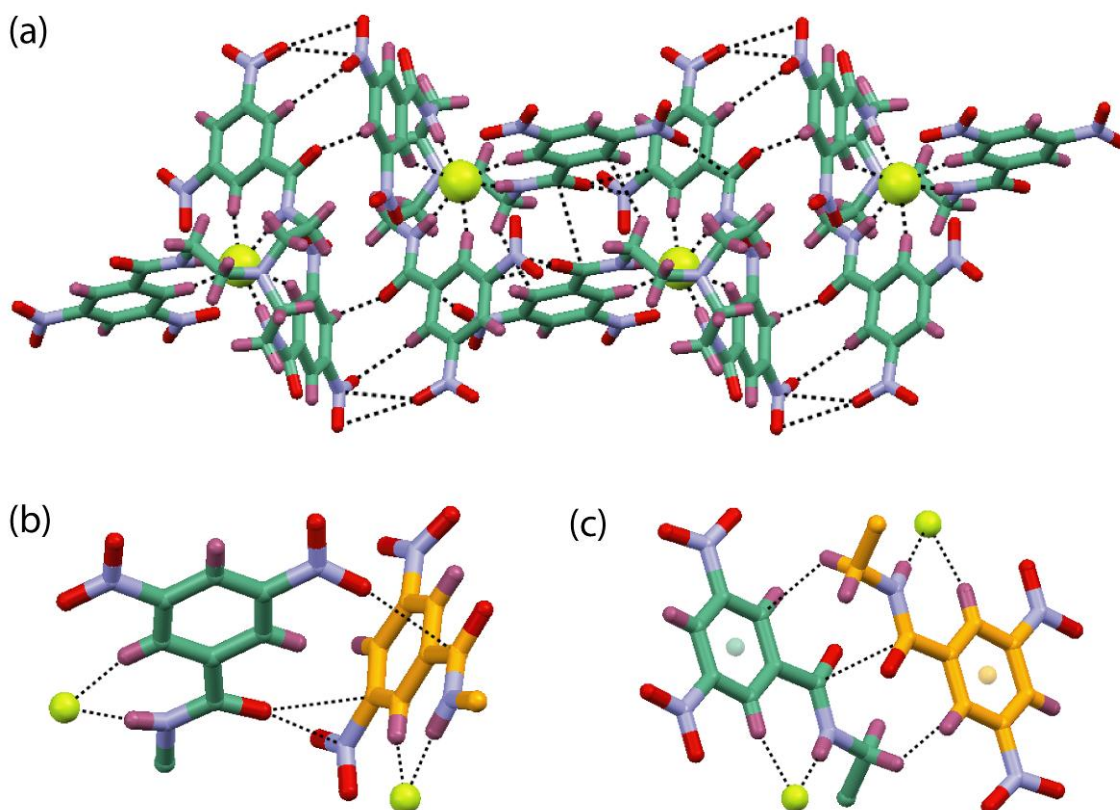


Figure S13. (a) H-bonding and electron donor-acceptor interactions ($n \rightarrow \pi^*/n \rightarrow \pi^*(k)$ and $\pi \rightarrow \pi^*$) between two F^- encapsulated receptor dimers. (b) Magnified view of the $n \rightarrow \pi^*$ ($O \rightarrow N/C$) interactions. (c) Magnified view of the aliphatic $C-H \cdots \pi$ and $\pi \rightarrow \pi^*$ ($C \rightarrow C$) interactions.

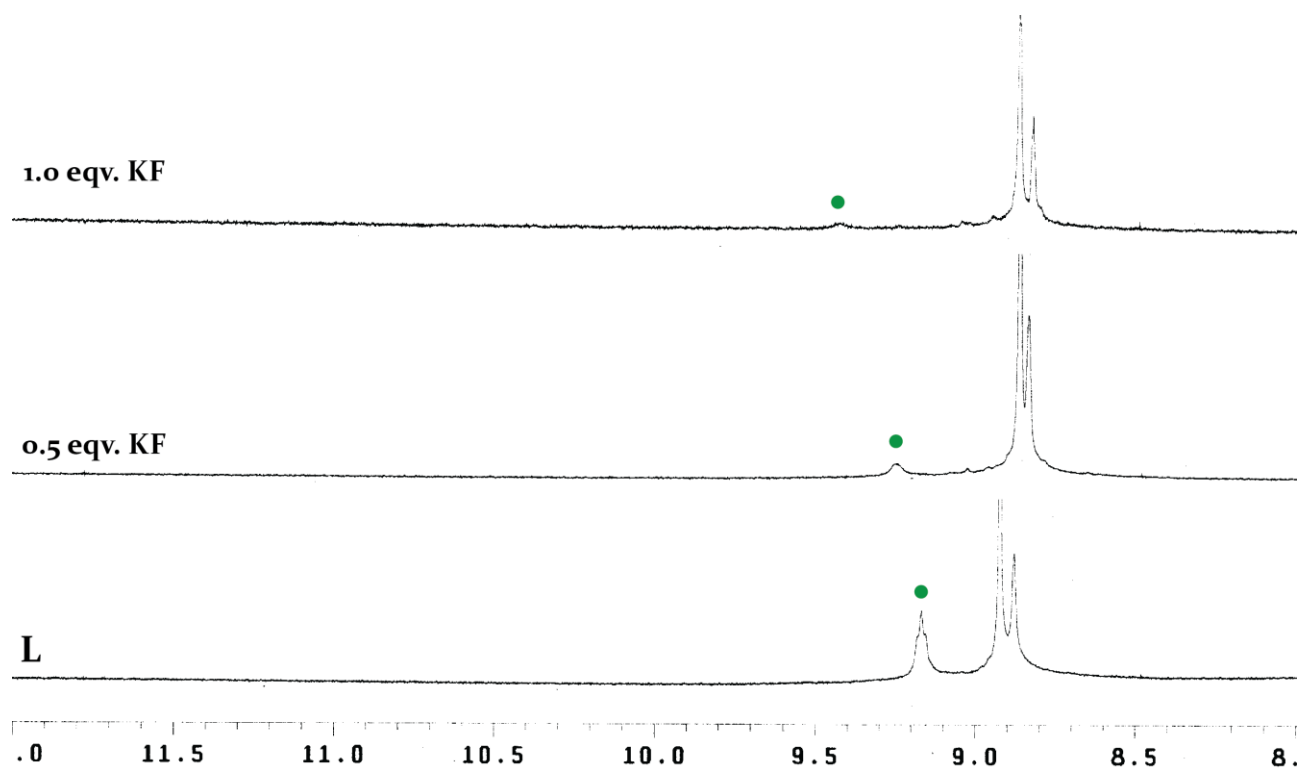


Figure S14. ^1H NMR titration of L with KF in $\text{DMSO-}d_6$ at 298 K, showing the downfield shift of amide $-\text{NH}$ protons up to 1 equiv. of KF beyond which precipitation occurs.